Aquatic Toxicology 184 (2017) 133–141

Contents lists available at ScienceDirect

Aquatic Toxicology

journal homepage: www.elsevier.com/locate/aquatox

Research Paper

Adverse effects of methylmercury (MeHg) on life parameters, antioxidant systems, and MAPK signaling pathways in the copepod *Tigriopus japonicus*

Young Hwan Lee[a,1], Hye-Min Kang[a,1], Duck-Hyun Kim[a], Minghua Wang[b], Chang-Bum Jeong[a,c,*], Jae-Seong Lee[a,*]

[a] Department of Biological Science, College of Science, Sungkyunkwan University, Suwon, 16419, South Korea
[b] Center for Marine Environmental Chemistry and Toxicology, College of the Environment & Ecology, Xiamen University, Xiamen, 361102, China
[c] Department of Chemistry, College of Natural Sciences, Hanyang University, Seoul, 04763, South Korea

ARTICLE INFO

Article history:
Received 9 December 2016
Received in revised form 17 January 2017
Accepted 18 January 2017
Available online 22 January 2017

Keywords:
MeHg
Methyl mercury
Reactive oxygen species
Copepod
Tigriopus japonicus
Antioxidant system
MAPK signaling pathway

ABSTRACT

Methylmercury (MeHg) is a concerning environmental pollutant that bioaccumulates and biomagnifies in the aquatic food web. However, the effects of MeHg on marine zooplankton are poorly understood even though zooplankton are considered key mediators of the bioaccumulation and biomagnification of MeHg in high-trophic marine organisms. Here, the toxicity of MeHg in the benthic copepod *Tigriopus japonicus* was assessed, and its adverse effects on growth rate and reproduction were demonstrated. Antioxidant enzymatic activities were increased in the presence of MeHg, indicating that these enzymes play an important role in the defense response to MeHg, which is regulated by a complex mechanism. Subsequent activation of different patterns of mitogen-activated protein kinase (MAPK) pathways was demonstrated, providing a mechanistic approach to understand the signaling pathways involved in the effects of MeHg. Our results provide valuable information for understanding the toxicity of MeHg and the underlying defense mechanism in response to MeHg exposure in marine zooplankton.

1. Introduction

In the aquatic environment, mercury is converted into various forms including metallic elements, inorganic salts, and organic compounds. Among these, organic mercury including methylmercury (MeHg) is known to have the highest toxicity among metals. Mercury is methylated to MeHg by sulfate-reducing bacteria and is subsequently taken up by microorganisms in the aquatic environment, resulting in biomagnification of up to 10,000-to 100,000-fold in high-trophic organisms (e.g., fish) compared to the concentration in the ambient water column (US EPA, 1997).

MeHg is a well-known neurotoxin, with particularly high toxicity in the nervous system (Clarkson et al., 2003) because it accumulates to high levels in astrocytes, which account for approximately 50% of the central nervous system (CNS), and both inhibits astrocytic uptake of glutamate and stimulates its efflux, leading to accumulation of glutamate in the extracellular fluid (Aschner, 1996; Aschner et al., 2000). This high concentration of glutamate stimulates N-methyl D-aspartate (NMDA)-type glutamate receptors, resulting in an increase in Na^+ and Ca^+ influx (Choi, 1992; Pivovarova and Andrews, 2010). The increased Ca^+ levels cause mitochondrial dysfunction with the generation of reactive oxygen species (ROS) (Atchison and Hare, 1994; Dreiem and Seegal, 2007). Thus, oxidative stress is closely linked to neurotoxicity and is considered a central event mediating MeHg-induced toxicity (Aschner et al., 2007). To date, there are several reports on MeHg-induced oxidative stress in invertebrates. For example, in the fruit fly *Drosophila melanogaster*, dietary MeHg exposure increased intracellular ROS levels and lipid peroxidation (Chauhan and Chauhan, 2016). In the nematode *Caenorhabditis elegans*, dietary exposure to 25 μM MeHg significantly increased the ROS level and mRNA expression level of glutathione *S*-transferase (*GST*) genes and led to developmental toxicity and neuron dysfunction (Vanduyn et al., 2010). MeHg is also known to cause adverse effects on growth and reproduction in an organism. For example, the fathead minnow *Pimephales promelas* female exposed to dietary MeHg exhibited retardation in reproduction and delayed spawning with inhibition

* Corresponding author at: Department of Biological Science, College of Science, Sungkyunkwan University, Suwon, 16419, South Korea.
E-mail addresses: cbjeong3@hanyang.ac.kr (C.-B. Jeong), jslee2@skku.edu (J.-S. Lee).
[1] These authors contributed equally to this work.

http://dx.doi.org/10.1016/j.aquatox.2017.01.010
0166-445X/

of gonadal development (Hammerschmidt et al., 2002; Drevnick and Sandheinrich, 2003). In the nematode *C. elegans*, significant developmental defects with 40% delayed time to adulthood have shown as a consequence of MeHg-induced oxidative stress (Vanduyn et al., 2010).

However, only a few studies have been conducted on the effects of MeHg on marine invertebrates despite their important ecological niche. In particular, among marine invertebrates, copepods are ecologically key species as they play an important role in the marine food chain, bridging the energy flow between primary producer and higher trophic organisms as an important food source (Lee et al., 2006; Pinto et al., 2001). Moreover, copepods have high relevance in laboratory experiments for ecotoxicological studies because of their high susceptibility to environmental toxicants, small body size (~1 mm), short life cycle (~2 weeks), ease of culture, and high reproductive rate (Raisuddin et al., 2007). In the present study, the benthic copepod *Tigriopus japonicus* was chosen as an experimental species based on these attractive aspects of copepods for ecotoxicological study.

We induced acute toxicity for 24 and 48 h to assess the toxicity of MeHg on *T. japonicus* and measured growth rate and fecundity in response to different concentrations of MeHg (0, 1, 10, 100, 500, and 1000 ng/L). Next, activities of antioxidant enzymes and their transcription levels were investigated to elucidate the defense mechanism against the elevated ROS levels in response to MeHg exposure. Furthermore, phosphorylation status was examined to determine whether mitogen-activated protein kinase (MAPK) pathways are involved in the defense against cellular damage induced by MeHg-mediated oxidative stress. The results of this study provide valuable information to better understand the responses of marine copepods to MeHg from the molecular to the organismal level.

2. Materials and methods

2.1. Culture and maintenance

The copepod *T. japonicus* was collected from a single rock pool at Haeundae beach (35°9′29.57”N, 129°9′36.60”E) in Busan (South Korea) in 2003, and maintained under controlled incubator conditions with a 12 h light/12 h dark cycle at a temperature of 25 °C. The salinity of the culture medium was 30 practical salinity units (psu) with pH 8.0. *T. japonicus* was fed a diet of *Chlorella* sp. (approximately 6×10^4 cells/mL) once a day. The identity of copepod species used for this experiment was verified by morphological characteristics and sequence analysis of *T. japonicus* mitochondrial cytochrome oxidase 1 (mt *CO1*) as the barcoding gene for animals (Ki et al., 2009).

2.2. Acute toxicity tests

The no observed effect concentration (NOEC) and half lethal concentration (LC50) at 48 and 96 h were evaluated to assess the acute toxicity of MeHg. Methyl mercury chloride (CH_3HgCl, analytical grade, molecular weight 251.08, purity >99.8%; cat. no. 33368) was purchased from Sigma-Aldrich (St. Louis, MO, USA). Ten male *T. japonicus* were exposed to 4 mL artificial sea water (ASW) containing different concentrations of MeHg (0, 1 [3.983 pM], 10 [39.828 pM], 100 [0.398 nM], 500 [1.991 nM], and 1000 ng/L [3.983 nM]) for 48 and 96 h under laboratory conditions and each treatment was performed in triplicate in 12-well culture plates (SPL Life Sciences, Seoul, South Korea). During the experiments, food was not supplied, and half of the media was renewed 48 h after exposure. Mortality was measured by examination under a stereomicroscope (SZX-ILLK200, Olympus Corporation, Tokyo, Japan) every 24 h, and a copepod was considered dead when it showed no sign of movement. Finally, NOEC, LC10, and LC50 values were calculated using Probit analysis (ToxRat Ver.2.09, Alsdorf, Germany, GmbH, 2005).

2.3. Growth rate and fecundity

Developmental time and fecundity were measured in *T. japonicus* exposed to 0, 1, 10, 100, 500, or 1000 ng/L MeHg. To examine retardation in developmental time, ovigerous females were initially collected and incubated in ASW for 2 h. Newborn nauplii were collected for *in vivo* experiments. Ten nauplii were transferred into 12-well culture plates with 4 mL ASW containing 0, 1, 10, 100, 500, or 1000 ng/L MeHg in triplicate. Developmental stages of nauplii in each exposure group were observed under a stereomicroscope (SZX-ILLK200, Olympus Corporation) every 24 h. The observation of nauplii was finished when all nauplii were matured, whereas observations on ovigerous females were continually performed to measure the fecundity.

To examine the effect of MeHg exposure on reproduction in *T. japonicus*, ten individual ovigerous females were transferred into 12-well culture plates and exposed to 0, 1, 10, 100, 500, or 1000 ng/L MeHg. Fecundity was measured by counting newborn nauplii every 24 h. During the experiments, half of the test media was renewed daily with green algae *Chlorella* sp. to maintain the copepods. All experiments were performed in triplicate, and temperature was maintained at 25 °C.

2.4. Measurement of reactive oxygen species (ROS) and glutathione (GSH) contents

To examine whether MeHg induces oxidative stress in the copepod *T. japonicus*, the intracellular ROS levels and GSH contents were measured after MeHg exposure (0, 1, 10, 100, 500, and 1000 ng/L). After MeHg exposure for 24 h, copepods (approximately 1000 individuals) were homogenized in a buffer containing 0.32 M sucrose, 20 mM HEPES, 1 mM $MgCl_2$, and 0.5 mM PMSF (pH 7.4) using a Teflon homogenizer. The homogenate was centrifuged at $3000 \times g$ for 20 min at 4 °C, and the supernatant was collected and used for measurements.

ROS level was measured using 2′,7′-dichlorodihydrofluorescein diacetate (H_2DCFDA; Molecular Probes, Eugene, OR, USA), which was oxidized to fluorescent dichlorofluorescein (DCF) by intracellular ROS. Black 96-well plates (SPL Life Sciences) were filled with phosphate-buffered saline (PBS), probe (H_2DCFDA at a final concentration of 40 μM), and the supernatant fraction to a final volume of 200 μL. Measurements were obtained at an excitation wavelength of 485 nm and emission wavelength of 520 nm using a spectrophotometer (Thermo™ Varioskan Flash, Thermo Electron, Vantaa, Finland).

Glutathione (GSH) concentration was determined enzymatically by measuring 5-thio-2-nitrobenzoic acid (TNB) as GSH cause a reduction of 5,5′-dithiobis(2-nitrobenzoic acid) (DTNB) to TNB. TNB was measured at an absorbance of 412 nm with a spectrophotometer (Thermo™ Varioskan Flash), and the level of GSH was calculated against standard curves generated using GSH equivalents (0, 150, and 350 μM).

The ROS and GSH levels were normalized to total protein as determined by the Bradford method (Bradford, 1976) and presented as percentage relative to control.

2.5. Measurement of GSH-related enzymatic activities

Glutathione peroxidase (GPx), glutathione reductase (GR), GST, and superoxide dismutase (SOD) activities were measured by using commercially available kits from Sigma-Aldrich. After exposure to

different concentrations (0, 1, 10, 100, 500, and 1000 ng/L) of MeHg for 24 h, *T. japonicus* (approximately 1000 individuals) was homogenized in cold buffer (50 mM Tris–HCl, 5 mM EDTA, and 1 mM 2-mercaptoethanol, pH 7.5) at a ratio of 1:4 (w/v) using a Teflon homogenizer. The homogenates were centrifuged at 10,000*g* for 10 min at 4 °C, and the upper aqueous layer containing the cytosolic fraction was collected for enzymatic assay according to the manufacturer's protocol.

The GPx and GR activity was indirectly determined by measuring NADPH consumption. *tert*-butyl hydroperoxide (*t*-Bu-OOH) was used as a substrate for GPx. During the reduction of t-Bu-OOH by GPx, oxidized GSH is generated which in turn reduced to GSH using NADPH as a reducing agent. The decrease in NADPH absorbance at 340 nm was measured with a spectrophotometer (Thermo^{TM} Varioskan Flash). In the case of GR, the decreased absorbance caused by the oxidation of NADPH during reduction of oxidized GSH by GR was measured at 340 nm.

GST activity was measured using 1-chloro-2,4-dinitrobenzene (CDNB) as a substrate. The enzymatic assay monitored the conjugation of CDNB and GSH by detection at 340 nm. Total SOD activity was measured by an enzymatic method using an SOD assay kit (Sigma-Aldrich). SOD activity was measured as an inhibition rate of the reduction of WST-1 (2-(4-Iodophenyl)-3-(4-nitrophenyl)-5-(2,4-disulfophenyl)-2H-tetrazolium, monosodium salt) that produce a water-soluble formazan dye upon reduction with a superoxide anion. The absorbance of WST-1 was measured at 440 nm.

Enzymatic activities were normalized by total protein and presented as% of control. Total protein was determined using the Bradford method (Bradford, 1976). All the experiments were performed in triplicate at 25 °C and absorbance was measured with a spectrophotometer (Thermo^{TM} Varioskan Flash).

2.6. Total RNA extraction and single-strand cDNA synthesis

Approximately 500 copepods were homogenized in five volumes of TRIZOL® reagent (Molecular Research Center, Inc., Cincinnati, OH, USA) with a tissue homogenizer and stored at −80 °C until RNA extraction. Total RNA was isolated according to the manufacturer's instructions. DNase I (Sigma-Aldrich, Inc.) was used to remove genomic DNA. Genomic DNA contamination was determined with 1% agarose gels with ethidium bromide and a UV transilluminator (Wealtec Corp., Sparks, NV, USA). Total RNA concentration was measured at 230, 260, and 280 nm (A230/260, A260/280) using a spectrophotometer (Ultrospec 2100 pro, Amersham Bioscience, Freiburg, Germany). RNA loaded within formaldehyde/agarose gels with ethidium bromide to check the quality of DNA the *18/28S rRNA* integrity and band ratio. Single-stranded cDNA was synthesized using 1 μg of RNA and reverse transcriptase (SuperScript^{TM} II RT kit, Invitrogen, Carlsbad, CA, USA) under the following condition; 65 °C/5 min, 42 °C/2 min, 42 °C/50 min, and 72 °C/15 min.

2.7. Real-time quantitative reverse transcriptase-polymerase chain reaction (qRT-PCR)

mRNA expression levels of *GST-D*, *GST-K*, *GST-M*, *GST-S*, *GST-T*, *GST-Z*, *mGST1*, *GST3*, *GR*, *GPx*, catalase (*CAT*), *CuZn-SOD*, and *Mn-SOD* genes in response to exposure to different concentrations (0, 1, 10, 100, 500, and 1000 ng/L) of MeHg for 24 h were measured by qRT-PCR (detailed information is appended in Table 1). All real-time qRT-PCR experiments were carried out in unskirted low 96-well clear plates (Bio-Rad, Hercules, CA, USA). Reaction conditions to detect specific PCR products were as follows: 94 °C/4 min; 35 cycles of 94 °C/30 s, 55 °C/30 s, 72 °C/30 s; and 72 °C/10 min. To confirm the amplification of specific products, cycles were continued to determine the melting curve under the following conditions: 95 °C/1 min, 55 °C/1 min, and 80 cycles beginning at 55 °C/10 s with a 0.5 °C increase per cycle. SYBR Green (Invitrogen, Carlsbad, CA, USA) was used to detect specific amplified products. Amplification and detection of SYBR Green-labeled products were performed using the CFX96 real-time PCR system (Bio-Rad). To set an appropriate reference gene for real-time RTPCR array, we validated the expression of ten reference candidates (*tubulin a*; glyceraldehyde 3-phosphate dehydrogenase, *gapdh*; *β-actin*; DNA-directed RNA polymerase II subunit RPB2, *polr2b*; glucose-6-phosphate dehydrogenase, *g6pd*; hypoxanthine phosphoribosyltransferase 1, *hprt1*; TATA box binding protein, *tbp*; elongation factor 1 α, *ef1α*; 18S ribosomal RNA, *18S rRNA*) that were used in our previous study as a preliminary experiment (Jeong et al., 2014a). As a result, the *ef1a* gene showed the most stable expression pattern in *T. japonicus* samples. No-template control reaction was included in every run for each primer pair. Data from each experiment were expressed relative to the expression level of the *ef1a* gene to normalize expression levels between samples. The fold change in relative gene expression was calculated by the $2^{-\Delta\Delta C}$T method (Livak and Schmittgen, 2001).

2.8. Western blot analysis

Polyclonal antibodies to phospho-SAPK/JNK (anti-rabbit, Thr-183/Tyr-185), ERK (anti-rabbit), and JNK (anti-rabbit) were obtained from Cell Signaling Technology (Beverly, MA, USA). Polyclonal antibodies to p38 MAPK (anti-rabbit), phospho-ERK1/2 (anti-mouse, Thr-202/Tyr-204), and phospho-p38 (anti-rabbit, Tyr-182) were purchased from Santa Cruz Biotechnology (Santa Cruz, CA, USA). Monoclonal antibodies to β-actin were obtained from Santa Cruz Biotechnology. Horseradish peroxidase (HRP)-linked anti-rabbit and anti-mouse antibodies were purchased from Cell Signaling Technology. The cross-reactivity of used antibodies in the present studies in *T. japonicus* has been validated via our preliminary experiments (Kang et al., in press).

T. japonicus (approximately 1000 individuals) were exposed to different concentrations of MeHg (0, 1, 10, 100, 500, and 1000 ng/L) in the 100 mL glass beaker for 24 h, and whole bodies were homogenized for extraction of proteins in lysis buffer (40 mM Tris–HCl [pH 8.0], 120 mM NaCl, 0.1% Nonidet-P40) containing a complete protease inhibitor cocktail (Roche, South San Francisco, CA, USA). Proteins (30 μg) were separated by 10% sodium dodecyl sulfate-polyacrylamide gel electrophoresis (SDS-PAGE) and transferred onto a nitrocellulose membrane (Amersham, Arlington Heights, IL, USA). The membrane was blocked with 2.5% bovine serum albumin (BSA) in Tris-buffered saline and incubated with primary antibodies (1:1000) overnight at 4 °C. The blots were developed with a peroxidase-conjugated secondary antibody (1:1000), and protein was visualized by enhanced chemiluminescence procedures (Amersham) according to the manufacturer's protocol.

2.9. Statistical analysis

Data were expressed as mean ± S.D. Significant differences were analyzed using one-way ANOVA followed by Tukey's test. $P < 0.05$ was considered significant. The SPSS ver. 17.0 software package (SPSS Inc., Chicago, IL, USA) was used for statistical analysis

3. Results

3.1. In vivo effects of MeHg exposure

The estimated values of NOEC, LC10, and LC50 of *T. japonicus* in response to MeHg were 3, 3.798, and 6.664 μg/L for 48 h exposure, respectively, and 2, 2.760, and 4.052 μg/L for 96 h exposure,

Table 1
Gene information and primers used for qRT-PCR.

Gene	Forward Primer (5′-3′)	Reverse Primer (5′-3′)	GenBank Accession Number
GST-D	CTCTGGCCGATTTATGCTTC	CAACTCGGTGAAACCAGACA	ACE81245
GST-K	AAACAGCAGCGCTTTTTGAC	GAGCTCATCATATTGCTCGTT	ACF06324
GST-M	TTTAGGAATGGCCTTGTTCG	AACCAAAGGCAGCCAAATAA	ACE81252
GST-S	ATGACTGGATTCGGATTTGGAC	GGCGTTTGGTCACATATTCGG	AAY89316
GST-T	GGTTCTCGGTTGGATCAATG	AGCATAAATCGGCCAGAGTC	ACE81253
GST-Z	AACCTTGGCTCGTTTCCAC	GTGGCAATCATGGAGTTCCT	ACE81250
mGST 1	TCCACTCCCGAGGATATTGA	ATCCTCCGGATTCTTTTCAC	ACE81248
mGST 3	CGGATTGGTTTGGACTCTTG	CACCTTGCATGCGTTTCTC	ACE81249
GR	CCATGACGGACAGAAAGCAGA	CTCCCATCTTGATGGCAACTC	ABG02425
GPx	TTTATGAGGCACGACTGTCCG	AAATTGGTTGCTCGGGAAAGC	AEQ35017
CAT	CACTGAGACCGGAAACCACG	TCGTCTCTGGTCAAATCGTCG	AEQ35015
CuZnSOD	ACTTTGGAACCTGGTCGCGAG	CCAATCGTGAGCCTGCGTTTC	AEM66981
MnSOD	GGTGGATCCGGTGAACCTGAA	CCGGCAGCCTTATTATAACCC	AEM66982
18S rRNA	TCGGGCTGTCTCGTTGGTGATTC	TGCCACAGTCGACAGTTGATAGG	EU054307

Table 2
LC10, LC50, 95% confidence intervals (CI), and No Observed Effect Concentrations (NOEC) for *T. japonicus* exposed to MeHg for 48 h and 96 h.

	NOEC (μg/L)	LC10 (95% CI; μg/L)	LC50 (95% CI; μg/L)
48 h	3	3.798 (3.376–4.272)	6.664 (5.005–8.873)
96 h	2	2.760 (1.593–3.260)	4.052 (3.501–5.053)

respectively (Table 2). The growth rate of *T. japonicus* was significantly delayed ($P < 0.05$) by MeHg in a concentration-dependent manner. Fecundity was also decreased ($P < 0.05$) in a concentration-dependent manner. Fecundity could not be measured at 1000 ng/L MeHg because there was no observable reproduction (Fig. 1).

3.2. Levels of ROS and GSH and enzymatic activities of GPx, GR, GST, and SOD

The intracellular ROS level was increased ($P < 0.05$) by MeHg in a concentration-dependent manner (Fig. 2A), whereas the GSH level was decreased at 500 and 100 ng/L MeHg (Fig. 2B).

Antioxidant enzymatic activities of GPx and GR were dose-dependently increased by exposure to MeHg. GST activity was also increased by MeHg up to a concentration of 100 ng/L, but decreased ($P < 0.05$) at 500 and 1000 ng/L MeHg. SOD activity was significantly decreased at 1000 ng/L ($P < 0.05$) (Fig. 3).

3.3. Transcription levels of antioxidant-related genes

Transcription levels of most antioxidant-related genes showed an increasing pattern ($P < 0.05$) at high concentrations of MeHg, whereas the expression level of *GPx* decreased ($P < 0.05$), showing a negative correlation with concentration of MeHg (Fig. 4). The detailed expression values are presented in **Fig. S1**.

3.4. Phosphorylation status of MAPKs

To investigate the phosphorylation status of the MAPK signaling pathway in response to MeHg in *T. japonicus*, we examined levels of phosphorylated ERK, JNK, and p38 compared to total expression levels. A decrease in the level of phosphorylated ERK was observed in the group exposed to 1000 ng/L MeHg. Phosphorylated JNK was significantly enhanced ($P < 0.05$) up to 100 ng/L MeHg and decreased after 500 and 1000 ng/L. However, the level of phosphorylated p38 was increased ($P < 0.05$) at 500 and 1000 ng/L MeHg (Fig. 5).

4. Discussion

Among marine copepods, *T. japonicus* has shown relative high tolerance to metals (Lee et al., 2007a; Lee et al., 2007b). For example, the LC50–48 h for cadmium, copper, and zinc was 25.2, 3.9, and 7.8 mg/L, respectively, for *T. japonicus* compared with less than 1 mg/L in other copepod species (Sullivan et al., 1983; Forget et al., 1998; Barka et al., 2001), indicating that *T. japonicus* is much less sensitive to these metals. The relatively high tolerance of *T. japoni-*

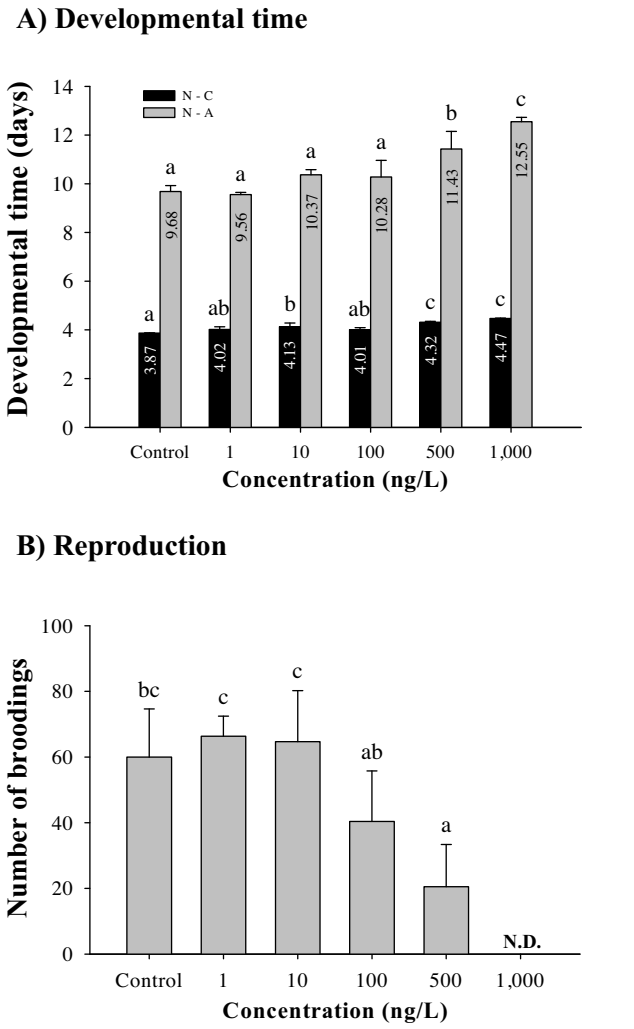

Fig. 1. Effects of exposure to different concentrations of MeHg on *T. japonicus* (A) growth rate and (B) reproduction. The black bar indicates the time taken from nauplius to copepodid stage (N-C), whereas the grey bar shows the time from nauplius to adult stage (N-A). Results represent the mean ± S.D. of three replicate samples. Differences between groups were analyzed for significance using Tukey's multiple comparison test. Different letters above columns indicate significant differences ($P < 0.05$).

Table 3
Comparison of MeHg and $HgCl_2$ toxicity between aquatic invertebrates.

Species	Mercury (II) chloride (Inorganic)		Methylmercury (Organic)		Reference
	Type of Acute Toxicity	Concentration (μg/L)	Type of Acute Toxicity	Concentration (μg/L)	
Tigriopus japonicus	N/A	N/A	Lethality (48 h) Lethality (96 h)	6.664 4.052	This study
Daphnia magna	Lethality (48 h)	1.5–14.8			Biesinger and Christensen (1972), Canton and Adema (1978), Barera and Adams (1983)
Daphnia pulex	Lethality (48 h)	2.2	Lethality (48 h) Lethality (96 h)	5.7 1.8	Canton and Adema (1978), Chen and McNaught (1992)
Mytilus edulis	Lethality (96 h)	161	NOEC (32 d)	0.3	Nelson et al. (1988), Pelletier (1988)
Argopecten irradians	Lethality (96 h)	89			Nelson et al. (1976)
Crepidula fornicata	Lethality (96 h)	60.0 (larvae) 330.0 (Adults)			Thain (1984)

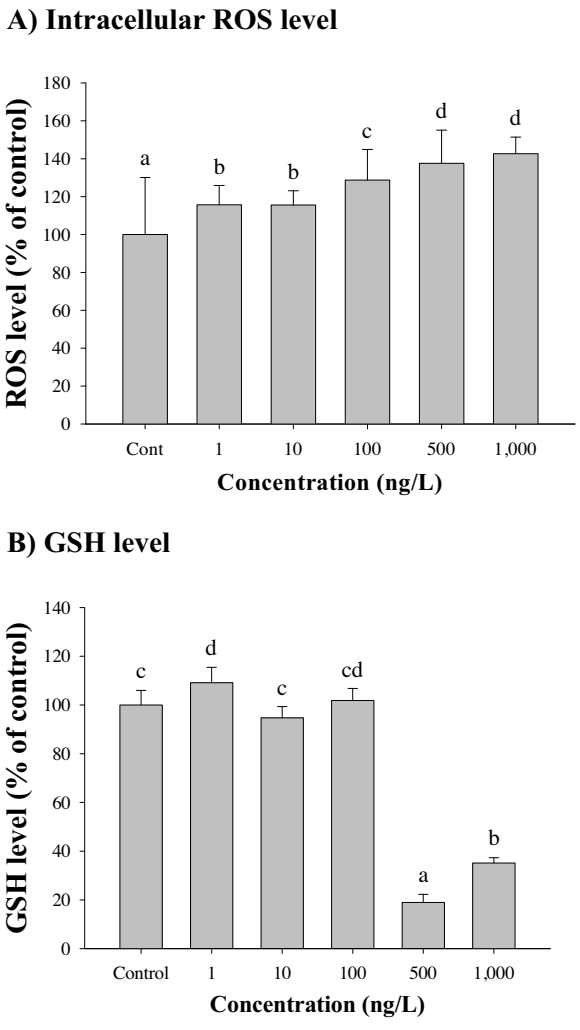

Fig. 2. Effects of exposure to different concentrations of MeHg on (A) intracellular ROS and (B) GSH level in *T. japonicus*. Levels of ROS and GSH are represented as percentage of controls. Results represent the mean ± S.D. of three replicate samples. Different letters above columns indicate significant differences ($P < 0.05$).

cus to metal, compared to other copepod species, can be explained by their efficient defense system (Rhee et al., 2013; Jeong et al., 2014b; Kim et al., 2014). However, *T. japonicus* exhibited very high sensitivity to MeHg compared with other metals, suggesting that MeHg has a distinct toxicity mechanism, although comparative analysis was not available due to a lack of acute toxicity reports of MeHg on marine copepod species. Evaluation of the toxicity of MeHg in several aquatic invertebrates showed higher toxicity compared with inorganic mercury (Table 3). MeHg is organic mercury that is highly lipophilic and tends to easily permeate cellular membranes, leading to cellular damage (Lakowicz and Anderson, 1980). Moreover, MeHg is known to form a complex with thiol groups and triggers enzyme inhibition (Hastings et al., 1975). The bioaccumulation of MeHg and subsequent alterations in biochemical homeostasis might explain the high toxicity of MeHg in *T. japonicus* compared with other metals.

Consistent with the results of acute toxicity, MeHg caused delays in developments and reproduction. Particularly, retardation was shown in early developmental stages (i.e., nauplius to copepodid) even at the lowest concentration tested (1 ng/L MeHg), whereas maturation (i.e., nauplius to adult) of *T. japonicus* was significantly delayed at higher concentrations of 500 and 1000 ng/L MeHg. Thus, 1 ng/L MeHg impairs the machinery of early developmental stages but not copepodid stages. In addition, exposure to 100–1000 ng MeHg resulted in a significant reduction in fecundity. Similarly, reductions in age-specific birth rates and reproduction were observed in *D. pulex* in response to 10 to 1000 ng/L MeHg (Doke et al., 2014). The negative effects of MeHg on growth rate, reproduction, and lifespan are likely explained by energy trade-off, as the limited energy budget may require reallocation of resources from development and reproduction in order to activate and maintain the defense system in response to toxicants (Won and Lee, 2014; Han et al., 2015).

The intracellular ROS levels were measured because the adverse effects of MeHg arise from oxidative stress, and ROS formation has been proposed as a biomarker of MeHg toxicity (Ali et al., 1992). In MeHg-exposed *T. japonicus*, ROS levels were significantly elevated in a concentration-dependent manner. In fact, increases in ROS levels are common phenomena in response to metal exposure and subsequently cause intracellular oxidative damage (Valko et al., 2005). For example, in the copepod *T. japonicus*, the ROS levels were dose-dependently increased with formation of apoptotic cells in response to copper exposure (Rhee et al., 2013). In the mussel *Crenomytilus grayanus*, cadmium exposure significantly caused

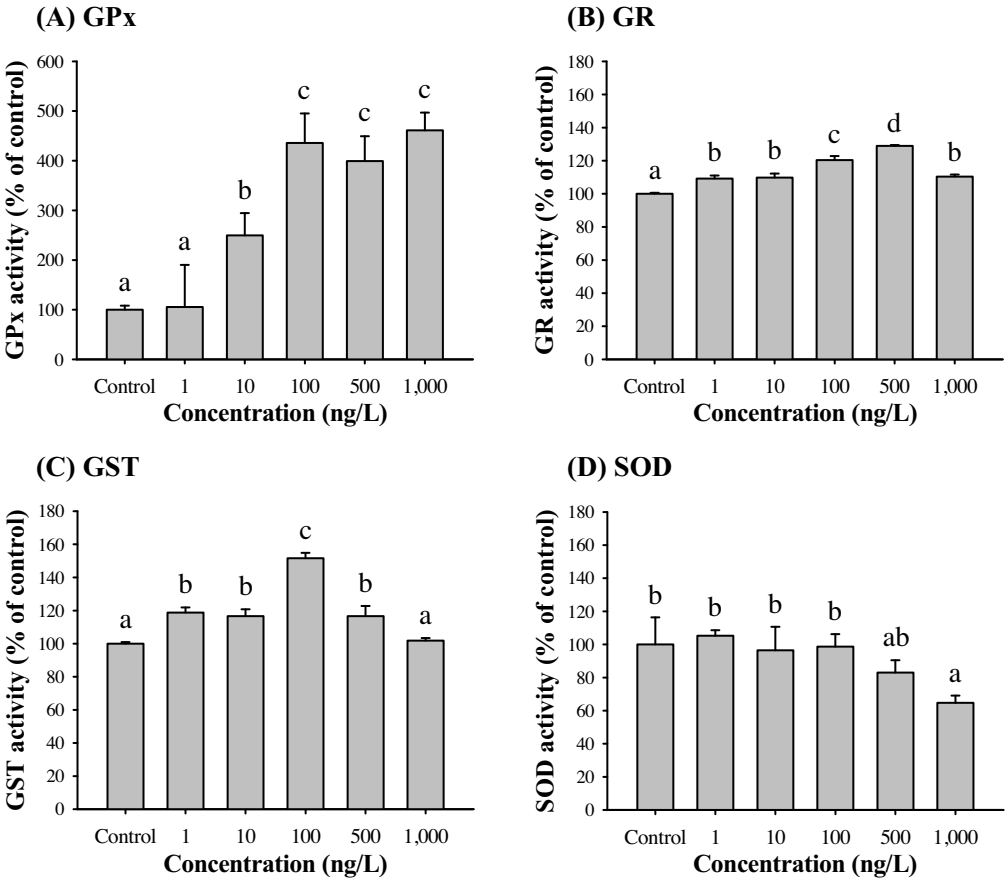

Fig. 3. Effects of exposure to different concentrations of MeHg on antioxidant-related enzymatic activities in *T. japonicus*: (A) GPx, (B) GR, (C) GST, and (D) SOD. Enzymatic activities are represented as percentage of controls. Results represent the mean ± S.D. of three replicate samples. Different letters above columns indicate significant differences ($P < 0.05$).

lipid peroxidation with ROS generation (Chelomin et al., 2005). Thus, MeHg-induced oxidative stress causes detrimental effects in *T. japonicus*.

GSH and its related enzymes are considered the most important defense system in response to oxidative stress (Halliwell and Gutteridge, 2007). In particular, GSH, a chelator for ROS scavenging, is considered a key molecule due to its involvement in detoxification. In *T. japonicus*, the GSH level was greatly decreased at 500 and 1000 ng/L MeHg. This could be explained by direct interaction of MeHg with the thiol group of GSH and formation of a GS-$HgCH_3$ complex (Ballatori and Clarkson, 1982), which decreases the GSH level. In mouse brain mitochondria, a decrease in GSH level was observed in response to MeHg exposure (Franco et al., 2007), as also shown in mouse neuron cells and glial cells (Kaur et al., 2006) and human non-neuronal cells (Amonpatumrat et al., 2008). The decreased GSH level in *T. japonicus* is likely linked to dysfunction of the GSH-related defense system, resulting in increased oxidative damage. This provides a potential clue to explain the *in vivo* toxicity and GSH level in response to 500 and 1000 ng/L MeHg.

Given the alteration of ROS and GSH levels in response to MeHg exposure, the antioxidant enzymatic activities of GPx, GR, GST, and SOD were measured. GSH-related antioxidant enzymes play a role in the central defense system in response to various environmental pollutants. For example, in *T. japonicus*, the antioxidant enzymatic activities of GPx, GR, GST, and SOD were shown to respond sensitively to various metals (e.g., silver, arsenic, cadmium, copper, and zinc) (Kim et al., 2014). In the rotifer *Brachionus koreanus*, involvement of GSH-related antioxidant enzymes in the response to benzo[a]pyrene exposure was reported (Kim et al., 2013). In the present study, GPx, GR, and GST activities in *T. japonicus* increased in a concentration-dependent manner up to 100 ng/L MeHg and slightly decreased at 500 and 1000 ng/L MeHg. Among these, the GPx activity was most highly increased. GPx is mainly involved in detoxification by oxidizing the reduced GSH, whereas GR is responsible for converting oxidized GSH into a reduced form, and the highly increased GPx activity suggests that GPx plays a central role in the detoxification process in response to MeHg. The highly increased activity of GPx functions as an effective antioxidant defense system in MeHg-induced oxidative stress and is also associated with a compensatory response of GST and SOD activities, which showed a negative correlation with GPx activity. SOD activity was inhibited at 500 and 1000 ng/L MeHg although there was no significant change at a low dose of MeHg. GST activity was dose-dependently increased until at 100 ng/L and then decreased at 500 and 1000 ng/L. The suppression of enzymatic activities shown in SOD and GST at high dose of MeHg may not be a merely compensatory regulation and also may represent the cellular damage in parallel to the result shown in our *in-vivo* toxicity experiments. In the case of GR, even though activity increased in a concentration-dependent manner up to 500 ng/L MeHg, the enzymatic activity was much lower than that of GPx and was not sufficient to convert GSSH to reduced GSH. Taken together, these results explain the depletion of GSH at a high concentration of MeHg exposure in *T. japonicus*.

Regarding the protective role of antioxidant enzymes, their gene expressions were mostly up-regulated in a concentration-dependent manner in response to MeHg exposure. Antioxidant genes in aquatic invertebrates have previously been proposed

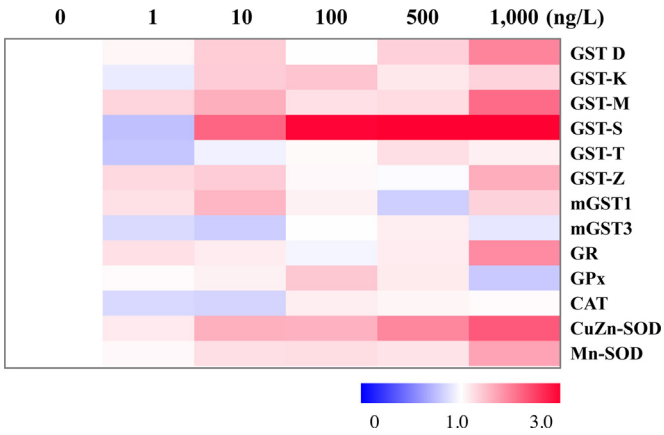

Fig. 4. Effects of exposure to different concentrations of MeHg on antioxidant-related gene expression in *T. japonicus*. Results represent the mean ± S.D. of three replicate samples.

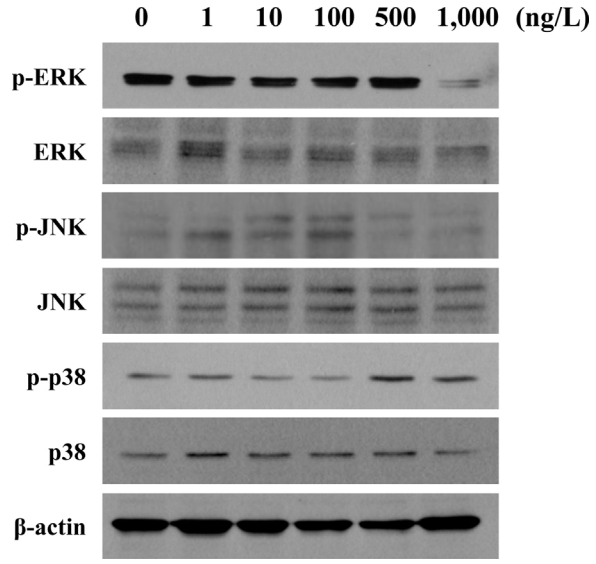

Fig. 5. Effects of exposure to different concentrations of MeHg on phosphorylation of MAPK signaling proteins in *T. japonicus*.

as biomarkers of the response to various environmental pollutants (Jemec et al., 2010; Rhee et al., 2013). In *T. japonicus*, *GST-S* responded most sensitively to MeHg exposure, as previously shown in Cu-exposed *T. japonicus* (Rhee et al., 2013), indicating that *GST-S* plays a central role in metal detoxification, with potential application as a biomarker for an early warning signal in metal pollution. In addition to *GST-S*, several *GST* isoforms including *GST-D* and *GST-M* in *T. japonicus* were also induced by MeHg exposure. In the mouse, 19 *GST* isoforms were identified in the mouse genome and showed different mRNA expression levels depending on the tissue and gender with some overlap (Knight et al., 2007), indicating that different isoforms of *GST* have distinct substrate specificity as suggested earlier (Mannervik and Danielson, 1988). While the function of GST-S in *T. japonicus* has been well characterized as a key antioxidant enzyme (Lee et al., 2007a; Lee et al., 2007b), the precise regulatory mechanism of other isoforms of GST is still unclear and further studies are required to speculate their function in detoxification. In the case of *SOD*, in contrast to its decreased enzymatic activity, the mRNA expression level was upregulated by MeHg in a concentration-dependent manner. A number of studies using Cu-exposed *T. japonicus* (Rhee et al., 2013) and the gamma-irradiated copepod *Paracyclopina nana* (Won and Lee, 2014) have shown a positive correlation between the transcription level and the activity level, whereas other studies have shown opposing results; for example, in mice exposed to ionizing irradiation (Hardmeier et al., 1997), in the renal cortex of streptozotocin-induced diabetic rats (Limaye et al., 2003), and in gamma-irradiated *T. japonicus* (Han et al., 2014). Thus, increased mRNA levels may not correspond to protein or activity level due to the low translational efficiency under oxidative stress (Ho et al., 1996). Activities of antioxidant enzymes are probably regulated via translational and post-translational regulatory mechanisms.

To investigate the signaling pathways of MeHg-mediated toxicity, the phosphorylation status of MAPK pathways in MeHg-exposed *T. japonicus* was examined. *T. japonicus* showed various expression patterns of MAPK pathways in response to MeHg exposure. The *p*-ERK level was exclusively decreased at 1000 ng/L MeHg without significant changes at lower concentrations. The phosphorylation patterns of JNK and p38 showed a negative correlation; *p*-JNK was activated at 0–100 ng/L MeHg, whereas the *p*-p38 level was increased at 500 and 1000 ng/L MeHg. The Western blot results supported the *in vivo* toxicity experiments in *T. japonicus* as the growth rate was most significantly delayed and reproduction was significantly decreased at 500 and 1000 ng/L MeHg. MAPK pathways are highly conserved across animal taxa and occupy a central position in various fundamental biological processes (McCubrey et al., 2006; Torii et al., 2006; Dhillon et al., 2007; Kang et al., 2017). Generally, the ERK signaling pathway is closely related to cell survival and proliferation, while JNK and p38 are involved in cell death processes (Matsuzawa and Ichijo, 2008; McCubrey et al., 2007; Wada and Penninger, 2004). Moreover, MAPK pathways are known as redox-sensitive pathways that are responsive to ROS (Bubici et al., 2006). Previous studies in the nematode *C. elegans* showed that phosphorylation of KGB-1, the JNK homologue, promotes reproduction, while PMK-1, the *p*-38 homologue, plays an opposite role in response to silver nanoparticle-induced oxidative stress (Lim et al., 2012; Gerke et al., 2014). Inhibition of the p38 signaling pathway suppressed cell death in a cadmium-treated human cell line, indicating the inductive role of p38 in cell death (Chuang et al., 2000). Blockage of the ERK signaling pathway using its specific inhibitor, U0126, inhibited worm pairing and reduced egg output (Ressurreição et al., 2014). In addition, MAPK pathways are also known to be closely related with defense system in response to oxidative stress. Previously, p38 has been activated with association of ROS induction by ultraviolet B radiation and copper exposure in *T. japonicus* (Rhee et al., 2013; Kim et al., 2015). Recently, in the copepod *P. nana*, nuclear factor erythroid 2-related factor 2 (NRF2), a key regulator of antioxidant genes (Itoh et al., 1997), was activated with *p*-ERK and *p*-p38 induction in response to nano-sized microbead-induced oxidative stress, indicating the *p*-ERK and *p*-p38 play the regulatory role in antioxidant system (Jeong et al., 2017). Taken together, these findings suggest that the decreases in *p*-ERK and *p*-JNK levels at 500 and 1000 ng/L MeHg are responsible for the retardation of reproduction, while the activation of *p*-p38 is likely involved in antioxidant system and cell death mechanism, thereby reducing the growth rate of *T. japonicus*.

In conclusion, our study clearly demonstrates the adverse effects of MeHg on the copepod *T. japonicus*. Growth rate and reproduction were retarded in response to MeHg-induced oxidative stress; subsequently, the transcription level and activities of antioxidant enzymes increased during the detoxification process. MAPK signaling pathways were differentially activated in concentration-dependent manners after MeHg exposure. To our knowledge, this is the first study on the adverse effects of MeHg in marine invertebrates, and our findings provide a better understanding of the potential impact of MeHg on the marine ecosystem.

Acknowledgements

This work was supported by a grant from the Development of Techniques for Assessment and Management of Hazardous Chemicals in the Marine Environment of the Ministry of Oceans and Fisheries, Korea funded to Jae-Seong Lee.

Appendix A. Supplementary data

Supplementary data associated with this article can be found, in the online version, at http://dx.doi.org/10.1016/j.aquatox.2017.01.010.

References

Ali, S.F., LeBel, C.P., Bondy, S.C., 1992. Reactive oxygen species formation as a biomarker of methylmercury and trimethyltin neurotoxicity. Neurotoxicology 13, 637–648.
Amonpatumrat, S., Sakurai, H., Wiriyasermkul, P., Khunweeraphong, N., Nagamori, S., Tanaka, H., Piyachaturawat, P., Kanai, Y., 2008. L-glutamate enhances methylmercury toxicity by synergistically increasing oxidative stress. J. Pharmacol. Sci. 108, 280–289.
Aschner, M., Yao, C.P., Allen, J.W., Tan, K.H., 2000. Methylmercury alters glutamate transport in astrocytes. Neurochem. Int. 37, 199–206.
Aschner, M., Syversen, T., Souza, D.O., Rocha, J.B., Farina, M., 2007. Involvement of glutamate and reactive oxygen species in methylmercury neurotoxicity. Braz. J. Med. Biol. Res. 40, 285–291.
Aschner, M., 1996. Methylmercury in astrocytes-what possible significance? Neurotoxicology 17, 93–106.
Atchison, W.D., Hare, M.F., 1994. Mechanisms of methylmercury-induced neurotoxicity. FASEB J. 8, 622–629.
Ballatori, N., Clarkson, T.W., 1982. Developmental changes in the biliary excretion of methylmercury and glutathione. Science 216, 61–63.
Barera, Y., Adams, W.J., 1983. Resolving some practical questions about Daphnia acute toxicity tests. In: Bishop, W.E., Cardwell, R.D., Heidolph, B.B. (Eds.), Aquatic Toxicology and Hazard Assessment. ASTM STP 802, American Society for Testing and Materials Philadelphia, PA, pp. 509–518.
Barka, S., Pavillon, J.F., Amiard, J.C., 2001. Influence of different essential and non essential metals on MTLP levels in the copepod *Tigriopus brevicornis*. Comp. Biochem. Physiol. C 128, 479–493.
Biesinger, K.E., Christensen, G.M., 1972. Effects of various metals on survival, growth, reproduction, and metabolism of *Daphnia magna*. J. Fish. Res. Bd. Can. 29, 1691–1700.
Bradford, M.M., 1976. A rapid and sensitive method for the quantitation of microgram quantities of protein utilizing the principle of protein-dye binding. Anal. Biochem. 72, 248–254.
Bubici, C., Papa, S., Pham, C.G., Zazzeroni, F., Franzoso, G., 2006. The NF-kappaB-mediated control of ROS and JNK signaling. Histol. Histopathol. 21, 69–80.
Canton, H., Adema, D.M.M., 1978. Reproducibility of short-term and reproduction toxicity experiments with *Daphnia magna* and comparison of the sensitivity of *Daphnia magna* with *Daphnia pulex* and *Daphnia cucullata* in short-term experiments. Hydrobiolgia 59, 135.
Chauhan, V., Chauhan, A., 2016. Effects of methylmercury and alcohol exposure in *Drosophila melanogaster*: potential risks in neurodevelopmental disorders. Int. J. Dev. Neurosci. 51, 36–41.
Chelomin, V.P., Zakhartsev, M.V., Kurilenko, A.V., Belcheva, N.N., 2005. An *in vitro* study of the effect of reactive oxygen species on subcellular distribution of deposited cadmium in digestive gland of mussel *Crenomytilus grayanus*. Aquat. Toxicol. 73, 181–189.
Chen, T.-Y., McNaught, D.C., 1992. Toxicity of methylmercury to *Daphnia pulex*. Bull. Environ. Contam. Toxicol. 49, 606–612.
Choi, D.W., 1992. Excitotoxic cell death. J. Neurobiol. 23, 1261–1276.
Chuang, S.M., Wang, I.C., Yang, J.L., 2000. Roles of JNK, and ERK mitogen-activated protein kinases in the growth inhibition and apoptosis induced by cadmium. Carcinogenesis 21, 1423–1432.
Clarkson, T.W., Magos, L., Myers, G.J., 2003. The toxicology of mercury-current exposures and clinical manifestations. New Engl. J. Med. 349, 1731–1737.
Dhillon, A.S., Hagan, S., Rath, O., Kolch, W., 2007. MAP kinase signaling pathways in cancer. Oncogene 26, 3279–3290.
Doke, D.A., Hudson, S.L., Dawson, J.A., Gohlke, J.M., 2014. Effects of early life exposure to methylmercury in *Daphnia pulex* on standard and reduced food ration. Reprod. Toxicol. 49, 219–225.
Dreiem, A., Seegal, R.F., 2007. Methylmercury-induced changes in mitochondrial function in striatal synaptosomes are calcium-dependent and ROS-independent. Neurotoxicology 28, 720–726.
Drevnick, P.E., Sandheinrich, M.B., 2003. Effects of dietary methylmercury on reproductive endocrinology of fathead minnows. Environ. Sci. Technol. 37, 4390–4396.
Forget, J., Pavillon, J.F., Menasria, M.R., Bocquene, G., 1998. Mortality and LC50 values for several stages of the marine copepod *Tigriopus brevicornis* (Müller) exposed to the metals arsenic and cadmium and the pesticides atrazine carbofuran, dichlorvos, and malathion. Ecotoxicol. Environ. Saf. 40, 239–244.
Franco, J.L., Braga, H.C., Stringari, J., Missau, F.C., Posser, T., Mendes, B.G., Leal, R.B., Santos, A.R., Dafre, A.L., Pizzolatti, M.G., Farina, M., 2007. Mercurial-induced hydrogen peroxide generation in mouse brain mitochondria: protective effects of quercetin. Chem. Res. Toxicol. 20, 1919–1926.
Gerke, P., Keshet, A., Mertenskötter, A., Paul, R.J., 2014. The JNK-like MAPK KGB-1 of *Caenorhabditis elegans* promotes reproduction, lifespan, and gene expressions for protein biosynthesis and germline homeostasis but interferes with hyperosmotic stress tolerance. Cell Physiol. Biochem. 34, 1951–1973.
Halliwell, B., Gutteridge, J., 2007. Free Radicals in Biology and Medicine, 4th edition. Oxford University Press Oxford, pp. 851.
Hammerschmidt, C.R., Sandheinrich, M.B., Wiener, J.G., Rada, R.G., 2002. Effect of dietary methylmercury on reproduction of fathead minnows. Environ. Sci. Technol. 36, 877–883.
Han, J., Won, E.-J., Lee, B.-Y., Hwang, U.-K., Kim, I.-C., Yim, J.H., Leung, K.M.Y., Lee, Y.S., Lee, J.-S., 2014. Gamma rays induce DNA damage and oxidative stress associated with impaired growth and reproduction in the copepod *Tigriopus japonicus*. Aquat. Toxicol. 152, 264–272.
Han, J., Won, E.-J., Lee, M.-C., Seo, J.-S., Lee, S.-J., Lee, J.-S., 2015. Developmental retardation, reduced fecundity, and modulated expression of the defensome in the intertidal copepod *Tigriopus japonicus* exposed to BDE-47 and PFOS. Aquat. Toxicol. 165, 136–143.
Hardmeier, R., Hoeger, H., Fang-Kircher, S., Khoschsorur, A., Lubec, G., 1997. Transcription and activity of antioxidant enzymes after ionizing irradiation in radiation-resistant and radiation-sensitive mice. Proc. Natl. Acad. Sci. U. S. A. 94, 7572–7576.
Hastings, F.L., Lucier, G.W., Klein, R., 1975. Methylmercury-cholinesterase interactions in rats. Environ. Health Perspect 12, 127–130.
Ho, Y.-S., Dey, M.S., Crapo, J.D., 1996. Antioxidant enzyme expression in rat lungs during hyperoxia. Am. J. Physiol. 270, L810–L818.
Itoh, K., Chiba, T., Takahashi, S., Ishii, T., Igarashi, K., Katoh, Y., Oyake, T., Hayashi, N., Satoh, K., Hatayama, I., Yamamoto, M., Nabeshima, Y., 1997. An Nrf2/small Maf heterodimer mediates the induction of phase II detoxifying enzyme genes through antioxidant response elements. Biochem. Biophys. Res. Commun. 236, 313–322.
Jemec, A., Drobne, D., Tisler, T., Sepcić, K., 2010. Biochemical biomarkers in environmental studies-lessons learnt from enzymes catalase, glutathione *S*-transferase and cholinesterase in two crustacean species. Environ. Sci. Pollut. Res. 17, 571–581.
Jeong, C.-B., Kim, B.-M., Lee, J.-S., Rhee, J.-S., 2014a. Genome-wide identification of whole ATP-binding cassette (*ABC*) transporters in the intertidal copepod *Tigriopus japonicus*. BMC Genom. 15, 651.
Jeong, C.-B., Kim, B.-M., Kim, R.-K., Park, H.G., Lee, S.-J., Shin, K.-H., Leung, K.M.Y., Rhee, J.-S., Lee, J.-S., 2014b. Functional characterization of P-glycoprotein in the intertidal copepod *Tigriopus japonicus* and its potential role in remediating metal pollution. Aquat. Toxicol. 156, 135–147.
Jeong, C.-B., Kang, H.-M., Lee, M.-C., Kim, D.-H., Han, J., Hwang, D.-S., Souissi, S., Lee, S.-J., Shin, K.-H., Park, H.G., Lee, J.-S., 2017. Adverse effects of microplastics and oxidative stress-induced MAPK/Nrf2 pathway-mediated defense mechanisms in the marine copepod *Paracyclopina nana*. Sci. Rep. 7, 41323.
Kang, H.-M., Jeong, C.-B., Lee, Y.H., Cui, Y.-H., Kim, D.-H., Lee, M.-C., Kim, H.-S., Han, J., Hwang, D.-S., Lee, S.-J., Lee, J.-S., 2017. Cross-reactivities of mammalian MAPKs antibodies in rotifer and copepod: application in mechanistic studies in aquatic ecotoxicology. Mar. Pollut. Bull., http://dx.doi.org/10.1016/j.marpolbul.2016.11.049, in press.
Kaur, P., Aschner, M., Syversen, T., 2006. Glutathione modulation influences methyl mercury induced neurotoxicity in primary cell cultures of neurons and astrocytes. Neurotoxicology 27, 492–500.
Ki, J.-S., Park, H.G., Lee, J.-S., 2009. The complete mitochondrial genome of the cyclopoid copepod *Paracyclopina nana*: a highly divergent genome with novel gene order and atypical gene numbers. Gene 435, 13–22.
Kim, R.-O., Kim, B.-M., Jeong, C.-B., Nelson, D.R., Lee, J.-S., Rhee, J.-S., 2013. Expression pattern of entire cytochrome P450 genes and response of defensomes in the benzo[α]pyrene-exposed monogonont rotifer *Brachionus koreanus*. Environ. Sci. Technol. 47, 13804–13812.
Kim, B.-M., Rhee, J.-S., Jeong, C.-B., Seo, J.S., Park, G.S., Lee, Y.-M., Lee, J.-S., 2014. Heavy metals induce oxidative stress and trigger oxidative stress-mediated heat shock protein (*hsp*) modulation in the intertidal copepod *Tigriopus japonicus*. Comp. Biochem. Phys. C 166, 65–74.
Kim, B.-M., Rhee, J.-S., Lee, K.-W., Kim, M.-J., Shin, K.-H., Lee, S.-J., Lee, Y.-M., Lee, J.-S., 2015. UV-B radiation-induced oxidative stress and p38 signaling pathway involvement in the benthic copepod *Tigriopus japonicus*. Comp. Biochem. Physiol. C 167, 15–23.
Knight, T.R., Choudhuri, S., Klaassen, C.D., 2007. Constitutive mRNA expression of various glutathione S-transferase isoforms in different tissues of mice. Toxicol. Sci. 100, 513–524.
Lakowicz, J.R., Anderson, C.J., 1980. Permeability of lipid bilayers to methylmercuric chloride: quantification by fluorescence quenching of a carbazole-labeled phospholipid. Chem.-Biol. Interact. 30, 309–323.
Lee, K.-W., Park, H.G., Lee, S.-M., Kang, H.-K., 2006. Effects of diets on the growth of the brackish water cyclopoid copepod *Paracyclopina nana* Smirnov. Aquaculture 256, 346–353.
Lee, K.-W., Raisuddin, S., Hwang, D.-S., Park, H.G., Lee, J.-S., 2007a. Acute toxicities of trace metals and common xenobiotics to the marine copepod *Tigriopus*

japonicus: evaluation of its use as a benchmark species for routine ecotoxicity tests in western Pacific coastal regions. Environ. Toxicol. 22, 532–538.
Lee, Y.-M., Lee, K.-W., Park, H., Park, H.G., Raisuddin, S., Ahn, I.-Y., Lee, J.-S., 2007b. Sequence, biochemical characteristics and expression of a novel sigma-class of glutathione *S*-transferase from the intertidal copepod, *Tigriopus japonicus* with a possible role in antioxidant defense. Chemosphere 69, 893–902.
Lim, D., Roh, J.-Y., Eom, H.-J., Choi, J.-Y., Hyun, J., Choi, J., 2012. Oxidative stress-related PMK-1 P38 MAPK activation as a mechanism for toxicity of silver nanoparticles to reproduction in the nematode *Caenorhabditis elegans*. Environ. Toxicol. Chem. 31, 585–592.
Limaye, P.V., Raghuram, N., Sivakami, S., 2003. Oxidative stress and gene expression of antioxidant enzymes in the renal cortex of streptozotocin-induced diabetic rats. Mol. Cell. Biochem. 243, 147–152.
Livak, K.J., Schmittgen, T.D., 2001. Analysis of relative gene expression data using real time quantitative PCR and the $2^{-\Delta\Delta C}$t method. Methods 25, 402–408.
Mannervik, B., Danielson, U.H., 1988. Glutathione transferases-structure and catalytic activity. CRC Crit. Rev. Biochem. 23, 283–337.
Matsuzawa, A., Ichijo, H., 2008. Redox control of cell fate by MAP kinase: physiological roles of ASK1-MAP kinase pathway in stress signaling. Biochim. Biophys. Acta 1780, 1325–1336.
McCubrey, J.A., Steelman, L.S., Abrams, S.L., Lee, J.T., Chang, F., Bertrand, F.E., Navolanic, P.M., Terrian, D.M., Franklin, R.A., D'Assoro, A.B., Salisbury, J.L., Mazzarino, M.C., Stivala, F., Libra, M., 2006. Roles of the RAF/MEK/ERK and PI3 K/PTEN/AKT pathways in malignant transformation and drug resistance. Adv. Enzyme Regul. 46, 249–279.
McCubrey, J.A., Steelman, L.S., Chappell, W.H., Abrams, S.L., Wong, E.W.T., Chang, F., Lehmann, B., Terrian, D.M., Milella, M., Tafuri, A., Stivala, F., Libra, M., Basecke, J., Evangelisti, C., Martelli, A.M., Fracnklin, R.A., 2007. Roles of the Raf/MEK/ERK pathway in cell growth, malignant transformation and drug resistance. Biochim. Biophys. Acta 1773, 1263–1284.
Nelson, D.A., Calabrese, A., Nelson, B.A., MacInnes, J.R., Wenzloff, D.R., 1976. Biological effects of heavy metals on juvenile scallops, *Argopecten irradians*, in short-term exposures. Bull. Environ. Contam. Toxicol. 16, 275–282.
Nelson, D.A., Miller, J.E., Calabrese, A., 1988. Effect of heavy metals on bay scallops, surf clams, and blue mussels in acute and long-term exposures. Arch. Environ. Contam. Toxicol. 17, 595–600.
Pelletier, E., 1988. Acute toxicity of some methylmercury complexes to *Mytilus edulis* and lack of selenium protection. Mar. Pollut. Bull. 19, 213–219.
Pinto, C.S.C., Souza-Santos, L.P., Santos, P.J.P., 2001. Development and population dynamics of *Tisbe biminiensis* (Copepoda: harpacticoida) reared on different diets. Aquaculture 198, 253–267.
Pivovarova, N.B., Andrews, S.B., 2010. Calcium-dependent mitochondrial function and dysfunction in neurons. FEBS J. 277, 3622–3636.
Raisuddin, S., Kwok, K.W.H., Leung, K.M.Y., Schlenk, D., Lee, J.-S., 2007. The copepod *Tigriopus:* A promising marine model organism for ecotoxicology and environmental genomics. Aquat. Toxicol. 83, 161–173.
Ressurreição, M., De Saram, P., Kirk, R.S., Rollinson, D., Emery, A.M., Page, N.M., Davies, A.J., Walker, A.J., 2014. Protein kinase C and extracellular signal-regulated kinase regulate movement, attachment, pairing and egg release in *Schistosoma mansoni*. PLoS Negl. Trop. Dis. 8, e2924.
Rhee, J.-S., Yu, I.T., Kim, B.-M., Jeong, C.-B., Lee, K.-W., Kim, M.-J., Lee, S.-J., Park, G.S., Lee, J.-S., 2013. Copper induces apoptotic cell death through reactive oxygen species triggered oxidative stress in the intertidal copepod *Tigriopus japonicus*. Aquat. Toxicol. 132, 182–189.
Sullivan, B.K., Buskey, E., Miller, D., Ritacco, P.J., 1983. Effects of copper and cadmium on growth, swimming and predator avoidance in *Eurytemora affinis* (Copepoda). Mar. Biol. 77, 299–306.
Thain, J.E., 1984. Effects of mercury on the prosobranch mollusc *Crepidula fornicata*: acute lethal toxicity and effects on growth and reproduction of chronic exposure. Mar. Environ. Res. 12, 285–309.
Torii, S., Yamamoto, T., Tsuchiya, Y., Nishida, E., 2006. ERK MAP kinase in G cell cycle progression and cancer. Cancer Sci. 97, 697–702.
US EPA, 1997. Mercury Study Report to Congress. Volume I Executive Summary, Vol. IV, An Assessment of Exposure to Mercury in the United States. US Environmental Protection Agency, Office of Air Quality Planning and Standards, and Office of Research and Development, Washington, DC, EPA/452/R-97-003.
Valko, M., Morris, H., Cronin, M.T., 2005. Metals, toxicity and oxidative stress. Curr. Med. Chem. 12, 1161–1208.
Vanduyn, N., Settivari, R., Wong, G., Nass, R., 2010. SKN-1/Nrf2 inhibits dopamine neuron degeneration in a *Caenorhabditis elegans* model of methylmercury toxicity. Toxicol. Sci. 118, 613–624.
Wada, T., Penninger, J.M., 2004. Mitogen-activated protein kinases in apoptosis regulation. Oncogene 23, 2838–2849.
Won, E.-J., Lee, J.-S., 2014. Gamma radiation induces growth retardation, impaired egg production, and oxidative stress in the marine copepod *Paracyclopina nana*. Aquat. Toxicol. 150, 17–26.